

# An offshore wind farm energy injection mastering using aerodynamic and kinetic control strategies.

Djamel Ikni<sup>1</sup>, Ahmed Ousmane Bagre<sup>2\*</sup>, Mamadou Bailo Camara<sup>1</sup>, and Brayima Dakyo<sup>1</sup>.

<sup>1</sup> Group of Research in Electrotechnics and Automatic of Le Havre (GREAH), University of Le Havre, France

<sup>2</sup> Laboratory of Renewable Energy and Energy Efficiency, International Institute for Water and Environmental Engineering -2iE Ouagadougou, Burkina Faso

**Abstract:** The injection of wind farm production into a grid, needs optimal strategies for energy transfer management. Usually, the power produced by the wind farms does not fulfil all the grid code requirements. The main problem is generally based on the way to reduce the impacts of power production fluctuations on the grid voltage and its frequency. To solve this problem, some authors suggest the use of an interface such as energy storage devices in order to compensate the wind power fluctuations. In fact, the storage devices installed between the wind farm and the grid can improve the power quality in terms of stability but in other hand the size and the cost of the system can be increased. In this paper, two solutions have been proposed in case the power quality produced by the wind farm is out of the grid code requirements. The improvement of the energy quality of an offshore wind farm without storage and connected to the grid is discussed. The proposed solution is to operate the wind turbines with a reserve of power. To distribute this reserve equitably among wind turbines, a proportional distribution algorithms has been developed. The results obtained show clearly the effectiveness of the strategy.

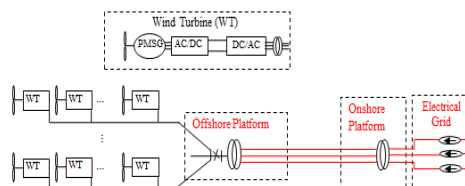
**Keywords:** Offshore wind farm, power fluctuation, wake effects, power management, grid code requirement.

## 1. Introduction

The European offshore wind power contribution in 2020 is estimated at 40% from the overall electric production from renewable sources. For the year 2020, the part of wind energy in the total energy production in Europe is predicted to be around 20% [1], [2]. In France, the part of wind energy in year 2017 estimated at 4,1% of the overall energy consumed [3] and for the year the target is to increase the renewable energy from 9.6% in 2005 to 23% in 2020 [4].

The rapid growth of wind energy worry grid managers because of its fluctuation behaviour in terms of power production. Moreover, these networks can achieve very rapidly significant wind energy penetration levels, as it's the case in three European countries: Denmark with 24.4%; Germany with 14.8% and Spain with 14.1% of the total capacity of the grid [5]. The estimated limit beyond which the fluctuations of wind power become very complex to manage, is between 20% and 30% [6]. In this context, all grid managers wish to limit the impacts of the power fluctuations for a better grid stability. These limits are generally summarized in grid codes [7]-[8]. Therefore, it is necessary to propose appropriate solutions in spite of the rapid growth of wind energy with the respect of power quality.

The main objective of this study is to evaluate the capacity of the wind farm to inject properly its production by using pitch angle control and inner inertial reserve. The first section is related to wind distribution model development in an offshore wind farm. The second section proposes some solutions for power quality improvement in the case the energy parameters are not compatible to the limits imposed in Germany's grid code used in this paper as a reference. The studied offshore wind farm system configuration is presented in Fig.1.



\* Corresponding author: [ahmed.bagre@2ie-edu.org](mailto:ahmed.bagre@2ie-edu.org)

**Fig. 1.** Topology of the studied offshore wind farm system .

**2. Wind distribution modelling for wind farm**

A critical point in the wind farm study is the wind distribution model. Many models have been developed in order to get their real behaviour, but unfortunately they need several parameters to be computed [9]-[10]. The proposed model takes into account the inequality distribution of the wind speed in the wind farm. This distribution is due to the strong interactions between wind speed and turbines positioned in first sectors in the direction of wind speed. These interactions cause wake effects which are considered in the model proposed. In [11] and [12], a simplified representation of wake effect is presented where, the wind speed diminished about 2-4% after each row/column of the farm. The same approach is used in the model proposed for wind distribution in wind farm. To reflect also the wind speed delay in the spread between the wind turbines, a delay function is added in wind speed model.

In [13] and [14], the authors have shown that when the wind direction is perpendicular to the lines of the wind farm, the power produced from the wind farm presents more fluctuations. The assumption made in this paper is that the wind speed is the same for all wind turbines positioned in the same line. The wind speed model for (i) line is presented in (1), where  $v_1$  is the wind speed for the first line ( $i=1$ ),  $dt_i$  is the delay function, and  $ds_i$  presents the wake effect.

These parameters depend on the wind farm configuration. The configuration is made to maximize the production and minimize the turbulence effect between downstream and upstream turbines. For this reason, an optimum distance between the wind turbines is necessary as described in [9] and [15]. This distance is roughly 7 times of wind turbine's diameter. The figure 2 shows the configuration of the wind farm studied with a power rated of 300MW. This power is produced by 60 Permanent Magnets Synchronous Generators (PMSG) linked to turbines. The generators are distributed in 10 lines, and each line includes 6 wind turbines which are in the same sector and submitted to the similar wind speed.

$$v_i = v_1(t - dt_i)(1 - ds_i) \tag{1}$$

The power produced by the wind farm is the sum of the contributions of all the turbines. These contributions are related to wind speeds profiles applied to each turbine. For this reason, it is necessary to calculate  $dt_i$  and  $ds_i$  parameters as is given in (2) and (3), respectively.

$$dt_i = \frac{7D}{v_{1mean}} i \tag{2}$$

$$ds_i = b_i \tag{3}$$

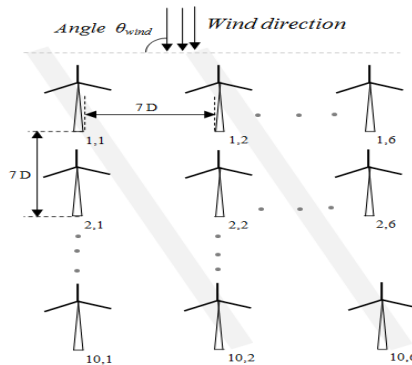


**Fig. 2.** Geometry of wind turbines positions in offshore wind farm.

Where,  $v_{1mean}$  is the average value of the wind speed for first line ( $i=1$ ),  $D$  presents the wind turbine diameter, and  $b$  is between 2% and 4%.  $b$  has been fixed at 2% in this paper. Using (2) and (3) in (1), the wind speed profile for each wind turbine can be estimated as presented in equation (4).

$$v_i = v_1(t - \frac{7D}{v_{1mean}} i)(1 - b_i) \tag{4}$$

The total power produced by the wind farm is given in (5), where  $P_i$  presents the power captured by the turbines of line  $i$ .  $P_i$  is as presented in (6), where,  $\rho$  is the air density ( $1.225kg/m^3$ );  $R$  is the radius of the rotor blade in (m) and  $C_{pmax}$  is the maximum power coefficient.

$$P_p = 6 \sum_{i=1}^{10} P_i \tag{5}$$

$$P_i = \begin{cases} \frac{1}{2} \rho \pi R^2 C_{pmax} v_i^3 & v_i \leq 11,5 \text{ m/s} \\ 5MW & v_i > 11,5 \text{ m/s} \end{cases} \quad (6)$$

**2.1. Wind speed model evaluation**

To evaluate the wind speed model, the wind speed profile for the first line turbines presented in Fig. 3 is used. The average value of this profile is around 10.05 m/s with the fluctuations of  $\pm 15\%$ . The wind speed model evaluation approach is based on a comparison between the wind farm power fluctuations with those extracted in real applications described in [16] and [17]. The method used to quantify power fluctuations, is based on the spectrum analysis of powers plotted in Fig. 4. The obtained spectres from computed power ( $P_p$ ) and reference ones ( $P_{ref}$ ) are illustrated in Fig. 5. The comparison criterion is based on an analysis of Fluctuation Harmonic Content (FHC) parameter. The FHC is equal to the Normalized Standard Deviation (NSD) of the power in the time domain described in [14]. FHC parameter can be estimated using (7), and where  $P_0$  is the produced power average value for 10 minutes,  $F$  presents the frequency interval. In this equation  $P(f)$  correspond to spectrum analysis of the power using Fast Fourier Transform (FFT).

$$FHC(F) = \frac{\sqrt{\sum_{f \in F} (P(f)/\sqrt{2})^2}}{P_0} \quad (7)$$

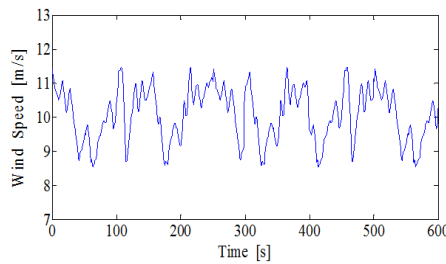


**Fig. 3.** Wind speed profile  $v_i$  for first line turbines.

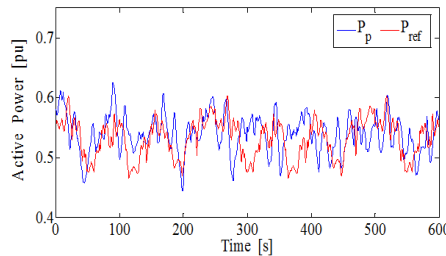


**Fig. 4.** Computed power compared  $P_p$  to measured power in real application  $P_{ref}$ .

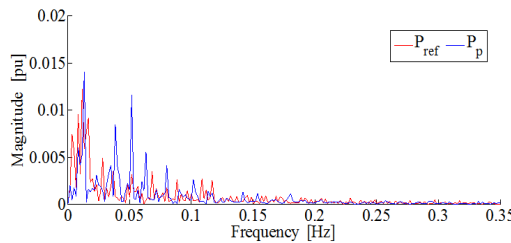


**Fig. 5.** Spectrum analysis of computed power and reference power.

The spectrum of each power is divided into three frequency domain:

- First domain is based on low frequencies which are lower than 0.01Hz.
- The second concerns the medium frequencies which are between 0.01 to 0.3Hz.
- The last zone corresponds to high frequencies which are above 0.3Hz.

FHC parameters estimated for Pref and Pp are summarized in (Table I).

**Table 1.** FHC parameters estimated for  $P_{ref}$  and  $P_p$

| Frequency                     | FHC of $P_{ref}$ | FHC of $P_p$ |
|-------------------------------|------------------|--------------|
| $f < 0.01\text{Hz}$           | 2.145            | 2.18         |
| $f \in [0.01 - 0.3\text{Hz}]$ | 2.37             | 2.4          |
| $f > 0.3\text{Hz}$            | 0.035            | 0.02         |
| Full region                   | 4.32             | 4.44         |

The estimated values of FHC in each zone are the same. The FHC values corresponding to high frequencies domain are negligible for two powers. For medium frequencies domain, FHC is about 2.37% for Pref, and 2.4% for Pp which presents a difference of 0.03%. In the case of low frequencies domain, the values of FHC are 2.145% for Pref, and 2.18% for Pp which correspond to a difference of 0.035%. These differences are very small and allows us to validate the model of the wind speed distribution proposed for wind farm application.

### 3. Energy quality compatibility problems between wind farm production and grid code exigencies

To inject energy from wind farm into the grid, the power from the wind farm must comply with the grid code requirements. In this paper, the requirements are focused on energy quality and power gradient ( $dP/dt$ )<sub>limit</sub>. These limits are fixed through the grid codes which are not the same for all the countries. For example, the power gradient limits fixed by countries such as Germany, Denmark and Nordic are shown in (Table 2).

**Table 2.** Power gradient limits extracted in [7]-[8]

| Grid code        | Power gradient (dP/dt)limit     |
|------------------|---------------------------------|
| E-on, Germany    | 10% of $P_{nom}$ per minute     |
| Eltra, Denmark   | 10-100% of $P_{nom}$ per minute |
| Nordic Grid Code | 10% of $P_{nom}$ per minute     |

To verify whether the power from the wind farm is compatible to the grid code requirement, the ratio given in (8) is used, where  $r$  presents 10% of rated power (0.5MW/s) and  $\tau_r$  is the sampling time in [s].

$$r = \frac{p_p(t+\tau_r) - p_p(t)}{\tau_r} \quad (8)$$

This equation is used to estimate the required power Pr profile for the grid using wind farm production Pp. The resulting profile which corresponds to the grid code requirement is presented in Fig. 6.

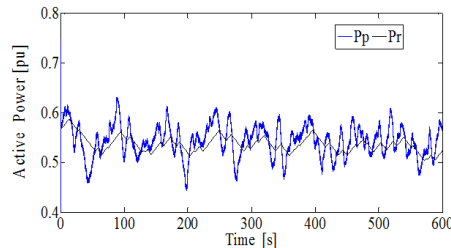


**Fig. 6.** Wind farm production  $P_p$  and required power profile for the grid  $P_r$ .

The figure 6 shows that, the wind farm production Pp has more fluctuations compared to the required power Pr of the grid. The difference between Pp and Pr must be compensated by control strategies, which is the main contribution of this paper. The strategies proposed are based on the downgrading operations of wind farm called in this paper as "power's reserve". These strategies enable to smooth the wind farm production in order to make at any time the total production becomes compatible to what is required for injection into the grid.

### 4. Wind farm power's reserve

The power's reserve in the wind farm can be obtained by reducing its power compared to its maximum capacity. Wind turbine operating in below its maximum power enables to create the power's reserve by action on the wind turbine speed or pitch angle. These actions allow obtaining a power's profile which satisfies the grid code requirements. Two control methods are possible to reduce the power from wind turbine through an action on power's coefficient  $C_p(\lambda, \beta)$  given in equation (9) [18].

$$\begin{cases} C_p(\lambda, \beta) = 0,73 \left( \frac{151}{\lambda_i} - 0,58 \beta - 0,02 \beta^{2,14} - 13,2 \right) \exp\left(\frac{18,4}{\lambda_i}\right) \\ \lambda_i = \frac{1}{\lambda - 0,02\beta} \frac{0,003}{\beta^3 - 1} \end{cases} \tag{9}$$

The first method is based on the acceleration and the deceleration of the wind turbine according to the profile needed. This technique enables to store energy in kinetic form. The second technique is related to pitch angle control which enables also to store energy in aerodynamic from.

#### 4.1. Kinetic reserve principle

For slower speeds than nominal ones, the wind turbine control optimizes the power by adjusting rotational speed. To describe the kinetic reserve principle, the pitch angle is assumed constant, so that, the power's coefficient  $C_p$  is the only parameter according to the rotational speed as illustrated in Fig. 7.

The kinetic reserve is obtained by a difference between the power estimated at  $\Omega_{tr-opt}$  and the one computed at  $\Omega_{tr-nominal}$ . This operation is getting by action on the electromagnetic torque of the generator [19]. The figure 8 shows the kinetic reserve ( $\Delta P_{IR-max}$ ) according to wind speed, which is limited to its nominal value of 11.5m/s. The maximum value of the kinetic reserve for each wind turbine can be estimated using (10). This equation shows that, the kinetic reserve is not proportional to the wind speed.

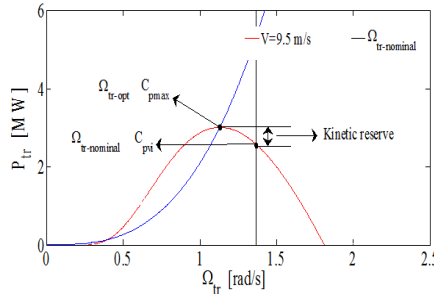


Fig. 7. Principle illustration of kinetic reserve.

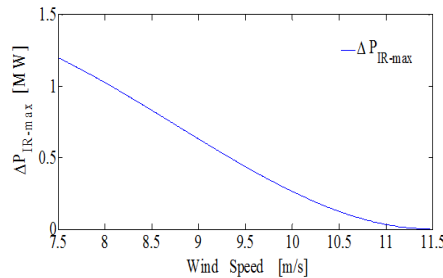


Fig. 8. Maximum kinetic reserve according to wind speed.

$$\begin{cases} \Delta P_{IR-max} = P_{tr}(C_{p_{v_i}}, \Omega_{tr-no\ min\ al}) - P_{tr}(C_{p_{max}}, \Omega_{tr-opt}) \\ C_{p_{v_i}} = f(\beta = 0, \lambda_v), \lambda_v = \frac{R \cdot \Omega_{tr-no\ min\ al}}{v} \end{cases} \tag{10}$$

**4.2. Aerodynamic reserve principle**

The pitch angle  $\beta$  control enables to reduce the power extracted from wind turbine by action on blades orientation. This solution can be used for all operation zone of the wind turbine as illustrated in Fig. 9 [20].

In normal operation, the pitch angle control limits the power captured by wind turbine at its nominal value. The increase of the Pitch angle reduces the lift of the blade which reduces the wind turbine torque and corresponding power as illustrated in Fig. 9. Whatever the wind speed, it is possible to act on the pitch angle to change the extracted power. The difference between available power in the wind and the power captured by the turbine after pitch angle action presents an aerodynamic reserve.

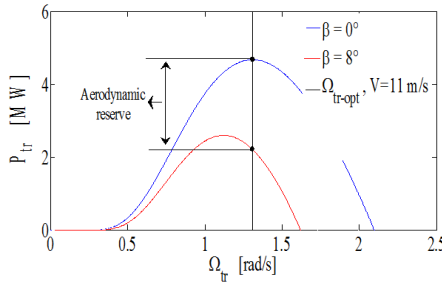


**Fig. 9.** Principle illustration of aerodynamic reserve.

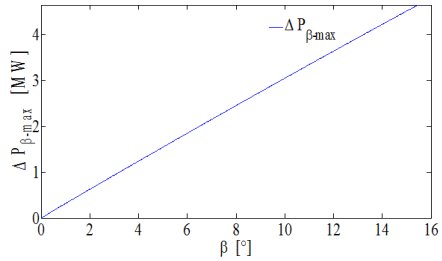


**Fig. 10.** Aerodynamic reserve according to pitch angle  $\beta$ , for a wind speed of 11 m/s.

The figure 10 shows that the aerodynamic reserve due to pitch angle variation can be significant. If necessary, this technique allows obtaining a power reserve equal to the maximum power that the turbine can extract from the wind. The operating point corresponds to the wind turbine feathering position. Aerodynamic reserve can be estimated as given in (11), where  $C_{pmax}$  is the maximum power coefficient without pitch angle,  $\Omega_{tr-opt-vi}$  presents optimal rotational speed corresponding to the wind speed of  $v_i$ , and  $C_{p\beta}$  presents power coefficient corresponding to a pitch angle value. In this technique, the generator’s rotational speed is fixed to its optimum value through the classical Maximum Power Point Tracking (MPPT) method.

$$\Delta P_{\beta-max} = P_{tr}(C_{pmax}, \Omega_{tr-opt}) - P_{tr}(C_{p\beta}, \Omega_{tr-opt-vi}) \tag{11}$$

**4.3. Required power profile estimation for the grid using “grid code” requirements**

The algorithm used to determine the required power reserve is given in Fig. 11. The aim of this algorithm is to calculate graphically the value of  $\alpha$  in order to get the power authorized for injection into the grid  $P_{r-ref}$  becomes less than the power available in the wind farm  $P_{p-avail}$ . This condition is obtained by adjusting the value of  $\alpha$  as presented in (13).

$$r = \frac{p'_{p-avail}(t+\tau_r) - p'_{p-avail}(t)}{\tau_r} \tag{12}$$

$$\begin{cases} P_{r-ref} - P_{p-avail} \leq 0 \\ P'_{p-avail} = \alpha P_{p-avail} \end{cases} \tag{13}$$

The relationship between  $R_p$ , the power reserve and  $\alpha$  coefficient is given in (14). The parameters estimated of the profile used to simulate the system are:  $R_p=17.5\%$  and  $\alpha$  is  $82.5\%$ . To smooth the available power  $P_{p-avail}$  of 319 MW, a power reserve of  $17.5\%$  necessary is nearly 56 MW.

$$R_p = 1 - \alpha \tag{14}$$

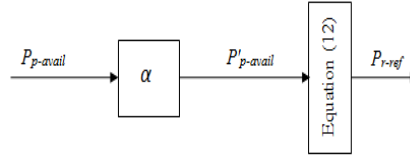


**Fig. 11.** Power required profile estimation for the grid.

**4.4. Aerodynamic reserve selection compared to kinetic reserve**

The maximum power reserve created using inertial technique increases when the wind speed decreases as shown in Fig. 8. The maximum reserve obtained with this method is about 19 MW which is lower than the required reserve of 56MW. Due to the poor performance of the inertial technique, the aerodynamic method is used in this paper to create the power reserve. As noted in section 4.2, this technique ensures the reserve regardless the wind speed and without any changes in the control strategy.

**4.5. Power reference sharing between wind turbines and PMSG control to operate with power reserve**

The method used for the power sharing between wind turbines is based on proportional distribution of the reserve as illustrated in (15). In this equation,  $P_{tr-i-avail}$  presents the maximum power of the turbine located on line  $i$ ,  $P_{p-avail}$  is the maximum power available in the wind farm,  $P_{r-ref}$  presents the required power profile for the grid which is imposed by the grid codes. The power reference distribution method is illustrated in Fig. 12.

$$P_{tr-i-ref} = \frac{P_{r-ref}}{P_{p-avail}} \cdot P_{tr-i-avail} \tag{15}$$

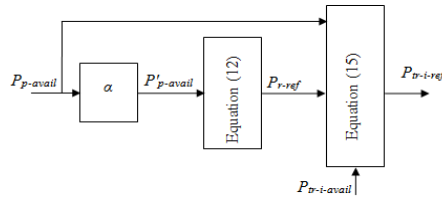


**Fig. 12.** Reserve distribution strategy in the wind farm.

The PMSG control strategy is based on the field-oriented control of the stator voltages [18]- [21] as illustrated in Fig. 13a. For the wind turbines operation with power’s reserve, PMSG speeds and the wind turbines power are controlled through pitch angle estimation method as illustrated in Fig. 13a. These control loops are the same for all the wind turbines in the same wind farm.

The first role of the inverter presented in Fig. 13b is to maintain the DC-bus voltage at a constant value. The second role is to control the reactive power exchanged with the grid. More information about the control strategy and PI controller parameters calculation can be found in [18]-[21].

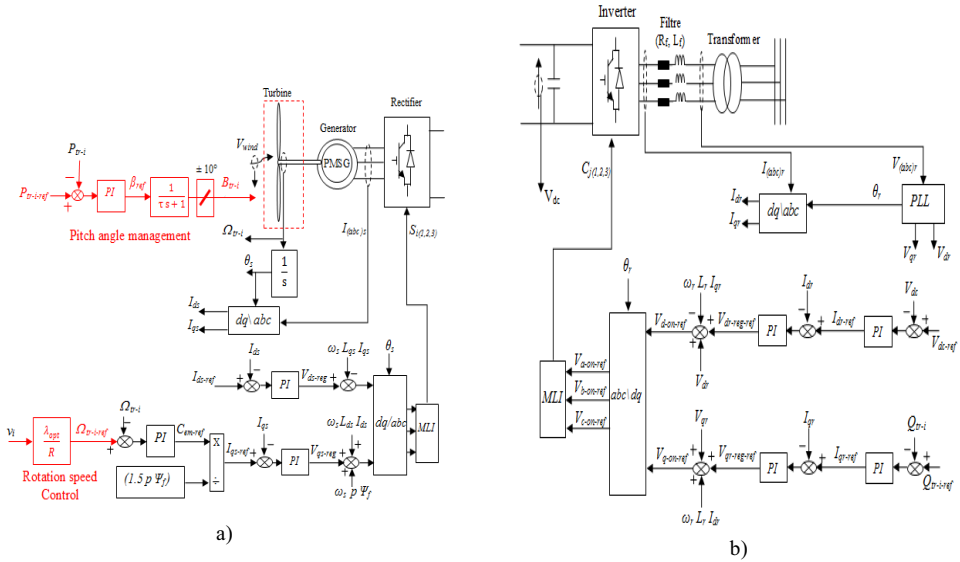


**Fig.13.a)** Wind generator control strategy **b)** Energy management method between PMSG and the grid.

**5. Simulation results**

The system simulation is done using Matlab\SimPowerSystem tools with the parameters given in appendix section. The contributions of three wind turbines located in lines 1, 5 and 10 are respectively shown in Fig. 14, 15 and 16. The curves are obtained using wind generator control strategy illustrated in Fig. 13b for each Permanent Magnet Synchronous Generators (PMSG) in the wind farm. The figures 14<sup>th</sup> to 16<sup>th</sup> show that the strategy control proposed gives a good expectation as the power controlled are close to the reference power. The difference between the potential power of the three wind turbines located in lines 1, 5 and 10 compared to the power respectively produced are presented in Fig. 17, Fig. 18 and Fig. 19. We can notice that, the power's reserve extracted from the wind turbine located in line 1 is larger than those of line 5 and 10 and the same thing can be seen for the wind turbines on line 5 and 10. This difference is due to the method used for the power sharing between the wind turbines which takes into account the wind speed for each wind turbine.

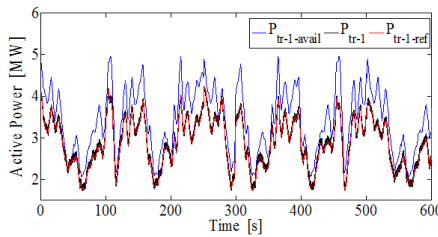


**Fig. 14.** Potential power of wind turbine located in line 1  $P_{tr-1-avail}$  compared to its real production  $P_{tr-1}$ .

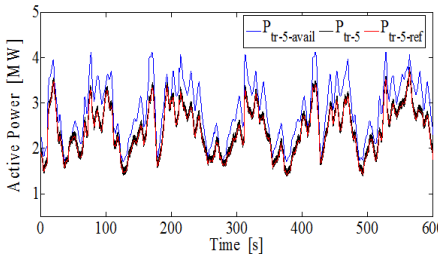


**Fig. 15.** Potential power of wind turbine located in line 5  $P_{tr-5-avail}$  compared to its real production  $P_{tr-5}$



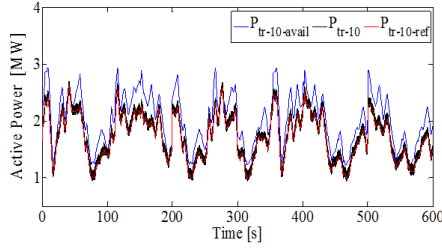


**Fig. 16.** Potential power of wind turbine located in line 1  $P_{tr-10-avail}$  compared to its real production  $P_{tr-10}$ .

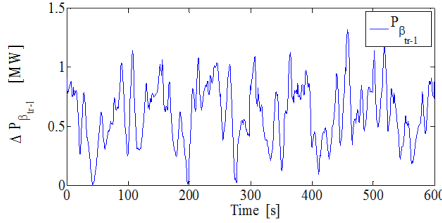


**Fig. 17.** Power's reserve extracted from wind turbine located in line 1.

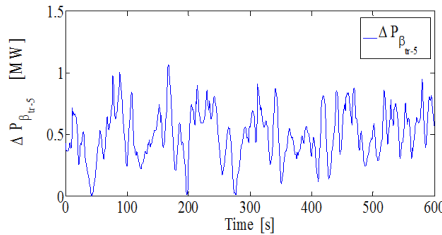


**Fig. 18.** Power's reserve extracted from wind turbine located in line 5.

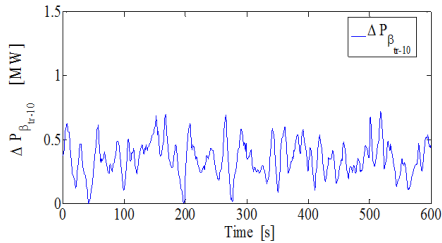


**Fig. 19.** Power's reserve extracted from wind turbine located in line 10.

The variations of the pitch angle for the wind turbines located in line 1, 5 and 10 are presented in Fig. 20. To analyze this last one,  $\gamma_{tr-i}$  is defined as the ratio between the output power and the available power for each wind turbine as expressed in (16). The  $\gamma_{tr-i}$  values for the three wind turbines are shown in Fig. 21. Its evolution is the same for the three wind turbines because the pitch angle variations are the same.

$$\gamma_{tr-i} = \frac{P_{tr-i-ref}}{P_{tr-i-avail}} \tag{16}$$

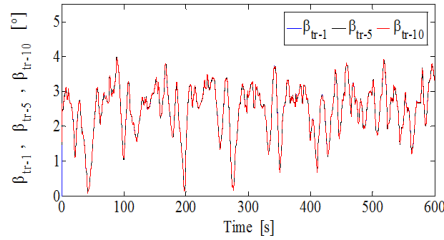


**Fig. 20.** Pitch angle variations for wind turbines located in line 1, 5 and 10.

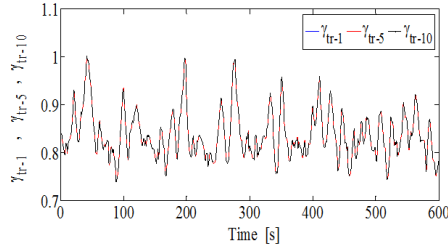


**Fig. 21.** Variation of ratio  $\gamma$ ,  $\gamma_{tr-1}$  for wind turbine 1,  $\gamma_{tr-5}$  for wind turbine 5 and  $\gamma_{tr-10}$  for wind turbine 10.

The power injected into the grid by the wind farm is presented in Fig. 22. This profile is adequate to the grid code requirements thank to the power's reserve based on aerodynamic approach performances as is illustrated in Fig. 23. The figure shows that the available power  $P_{p-avail}$  is more fluctuating compared to the power injected into the grid  $P_r$ . In other terms, the aerodynamic reserve enables the wind turbines to condition their productions so that, the wind farm production becomes acceptable to the grid code requirements.

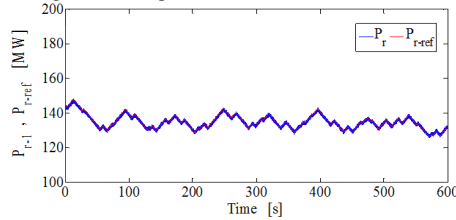


**Fig. 22.** Power injected into the grid from the wind farm.

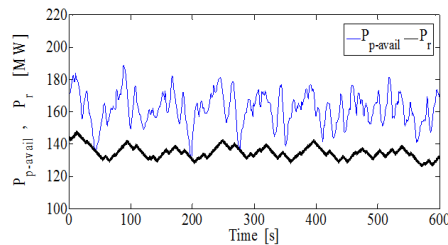


**Fig. 23.** Available power in the wind farm  $P_{p-avail}$  compared to the power injected into the grid  $P_r$ .

## 6. Conclusion

In this paper, a wind distribution model in the wind farm is proposed and evaluated by comparing the simulation results to the real data extracted from literature. Subsequently, an analysis of the quality of the energy produced by a wind farm is done with the goal to compare the rate of power fluctuations to what is currently admitted by E-on Germany grid code used in this study as a reference. The comparison is done by using the FHC factor.

The wind turbines operations with power's reserve enables to produce energy with the desired fluctuations rate. To create this reserve, an analysis of the wind turbine ability shows that there are two possible solutions. The first is based on inertial approach and the second is focused on aerodynamic method through the pitch angle estimation. The

comparison of the two approaches shows that, the aerodynamic method is the best. The power reserve sharing between wind turbines is based on proportional distribution algorithms. The simulation results shows that, the strategy proposed is adequate. In other words, the wind farm is able to smooth its production by functioning with power's reserve. The most disadvantages of this strategy is that the wind farm is under exploitation and besides, we have the mechanical fatigue of the turbine due to recurrent vibrations of the blades.

## References

- [1] T.R. Ayodele, A.A. Jimoh, J.L Munda, J.T Agee, " *Challenges of grid integration of wind power on power System grid integrity: A Review*", International journal of renewable energy research (IJRER), **Vol.2, No.4**, (2012).
- [2] J.Wilkes, I.Pineda, G. Corbetta, " *Wind energy scenarios for 2020*", European wind energy association (EWEA), technical report, (July 2014).
- [3] RTE, Syndicat des énergies renouvelable, Enerdis, ADEef, " *Panorama de l'électricité solaire au 31 mars 2017*", (March 2017).
- [4] J. Kabouris and F. D. Kanellos, " *Impacts of large-scale wind penetration on designing and operation of electric power systems*", Sustainable Energy, IEEE Transactions on, **Vol. 1, No.2**, pp.107-114, (2010).
- [5] Ministry of Ecology, Energy, Sustainable Development and the Sea, " *National Action Plan for renewable energies (in French)*", **Article 4** of Directive 2009/28 / EC of the European Union, (2009).
- [6] I.Pineda, S.Azau, J.Moccia and J.Wilkes, " *Wind in power 2013: European statistics*", European wind energy association (EWEA), technical report, (February 2014).
- [7] Ministry of Ecology, Sustainable Development and Energy, " *Wind power and photovoltaics: energy issues, industrial and societal (in French)* ", technical report, (September 2012).
- [8] M. Tsili and S. Papathanassiou, " *A review of grid code technical requirements for wind farms*", IET Renewable Power Generation, **Vol.3, No.3**, pp 308–332, (2009).
- [9] A. H. Kassem, El-Saadany E.F, El-Tamaly H.H. and Wahab M.A.A., " *Ramp rate control and voltage regulation for grid directly connected wind turbines*", Power and Energy Society General Meeting - Conversion and Delivery of Electrical Energy in the 21<sup>st</sup> Century, 2008 IEEE, Pittsburgh, PA, USA, July 20-24, (2008).
- [10] X.Han, Y.Qu, P.Wang and I. Yang, " *Four-dimensional wind speed model for adequacy assessment of power systems with wind farms*", Power Systems, IEEE Transactions On, **Vol.28, No.3**, pp. 2978-2985, (2013).
- [11] J.Park, K.H. Law, " *Cooperative wind turbine control for maximizing wind farm power using sequential convex programming*", Energy Conversion and Management, **Vol.101, No.1**, pp.295–316, (2015).
- [12] H. K. Vladislav Akhmatov, " *An aggregate model of a grid-connected, large-scale, offshore wind farm for power stability investigations - importance of windmill mechanical system*", International Journal of Electrical Power & Energy Systems, **Vol.24, No.9**, pp.709-717, 2002.
- [13] C.E. Băncăanu, V.Iulian, " *Coordinated control of wind turbines*", Master thesis, Department of Energy Technology - Pontoppidanstræde 101, Aalborg University, Denmark, June (2011).
- [14] N. A. Kallioras, N.D. Lagaros, M.G. Karlaftis, P.Pachy, " *Optimum layout design of onshore wind farms considering stochastic loading*", Advances in Engineering Software, **Vol.88**, pp. 8–20, (2015).
- [15] W. Li, G. Joos and C. Abbey, " *Wind power impact on system frequency deviation and an ESS based power filtering algorithm solution*", IEEE Power Systems Conference and Exposition, **PSCE '06**, 2006 IEEE PES, Atlanta GA, USA, October 29 -November 1, (2006).
- [16] W.Li, " *An embedded energy storage system for attenuation of wind power fluctuations*", Ph.D. dissertation, Department Electrical Engineering, McGill University, Montreal, Canada, May (2010).
- [17] E. Spahić and G. Balzer, " *The impact of the wind farm size on the power output fluctuation*", European Wind Energy Conference (EWEC), Athens, Greece, February (2006).
- [18] M.Singh, V.Gevorgian, E.Muljadi, E.Ela, " *Variable-speed wind power plant operating with reserve power capability*", Energy Conversion Congress and Exposition (ECCE), 2013 IEEE, Denver, USA, September 15-19, (2013).
- [19] M. Jannati, S.H.Hosseiniyan, B.Vahidi, Guo-JieLi, " *A survey on energy storage resources configurations in order to propose an optimum configuration for smoothing fluctuations of future large wind power plants*", Renewable and Sustainable Energy Reviews, **Vol.29**, pp. 158–172, (2014).

- [20] Z. Zhou, F. Sculler, J.F. Charpentier, M.E.H. Benbouzid and T. Tang," *Power smoothing control in a grid-connected marine current turbine system for compensating swell effect*", IEEE Transactions on Sustainable Energy, **Vol.4, No. 3**, pp. 816-826, (2013).
- [21] D. Ikni, M.S. Camara, M.B. Camara , B. Dakyo, H. Gualous, " *Permanent Magnet Synchronous Generators for Large Offshore Wind Farm Connected to Grid - Comparative Study between DC and AC Configurations*", International journal of renewable energy research (IJRER), **Vol.4 ,No.2**, (2014).